Journal of Clinical and Translational Hepatology **2023**
DOI: 10.14218/JCTH.2022.00401

Original Article

Dysregulation of PLOD2 Promotes Tumor Metastasis and Invasion in Hepatocellular Carcinoma

Keren Li[1,2#], Yi Niu[1#], Kai Li[1,2], Chengrui Zhong[1,2], Zhiyu Qiu[1,2], Yichuan Yuan[1,2], Yunxing Shi[1,2], Zhu Lin[1,2], Zhenkun Huang[1,2], Dinglan Zuo[1], Yunfei Yuan[1,2*] and Binkui Li[1,2*]

[1]*State Key Laboratory of Oncology in South China, Sun Yat-Sen University Cancer Center, Guangzhou, Guangdong, China;* [2]*Department of Liver Surgery, Sun Yat-Sen University Cancer Center, Guangzhou, Guangdong, China*

Received: 18 August 2022 | **Revised:** 4 December 2022 | **Accepted:** 22 February 2023 | **Published online:** 21 April 2023

Abstract

Background and Aims: Metastasis is a major factor associated with high recurrence and mortality in hepatocellular carcinoma (HCC) patients while the underlying mechanism of metastasis remains elusive. In our study, procollagen-lysine, 2-oxoglutarate 5-dioxygenase 2 (PLOD2) was shown to be involved in the process of metastasis in HCC. ***Methods:*** The Cancer Genome Atlas (TCGA) database and HCC tissue microarrays were used to evaluate the expression of genes. *In vitro* migration, invasion, *in vivo* subcutaneous tumor model and *in vivo* lung metastasis assays were used to determine the role of PLOD2 in tumor growth and metastasis in HCC. RNA sequencing and gene set enrichment analysis were performed to uncover the downstream factor of PLOD2 in HCC cells. A luciferase reporter assay was performed to evaluate the interaction between PLOD2 and interferon regulatory factor 5 (IRF5). ***Results:*** The expression of PLOD2 in HCC tissues was higher than that in adjacent tissues, and increased PLOD2 expression was often found in advanced tumors and was correlated with poor prognosis in HCC patients. *In vitro* experiments, knockdown of PLOD2 reduced the migration and invasion of human HCC cells. Loss of PLOD2 suppressed human HCC growth and metastasis in a subcutaneous tumor model and a lung metastasis model. Baculoviral IAP repeat containing 3 (BIRC3) was proven to be the downstream factor of PLOD2 in human HCC cells. In addition, PLOD2 was transcriptionally regulated by IRF5 in HCC cells. ***Conclusions:*** High expression of PLOD2 was regulated by IRF5, which was correlated with the poor survival of HCC patients. PLOD2 enhanced HCC metastasis via BIRC3, suggesting that PLOD2 might be a valuable prognostic biomarker for HCC treatment.

Citation of this article: Li K, Niu Y, Li K, Zhong C, Qiu Z, Yuan Y, *et al*. Dysregulation of PLOD2 Promotes Tumor Metastasis and Invasion in Hepatocellular Carcinoma. J Clin Transl Hepatol 2023. doi: 10.14218/JCTH.2022.00401.

Introduction

Hepatocellular carcinoma (HCC) is the main type of liver cancer. It has a poor prognosis and ranks as the fourth leading cause of cancer-related death worldwide.[1] Due to the lack of effective treatment, the 5-year overall survival of HCC patients is less than 20%.[2,3] The high mortality of patients with advanced HCC is often due to metastasis. However, there is little knowledge about the underlying mechanisms of metastasis and invasion in HCC. Thus, a better understanding of the molecular mechanisms of metastasis in HCC may help us explore novel diagnostic and therapeutic strategies for HCC treatment. Collagen has an important role in the migration, invasion and proliferation of cancer cells.[4,5] Previous studies have suggested that different covalent collagen cross-links enhance the accumulation of stabilized collagen in many kinds of human cancers, which is related to poor patient survival.[6,7] Procollagen-lysine, 2-oxoglutarate 5-dioxygenase 2 (PLOD2) is a key enzyme promoting the formation of stabilized collagen cross-links.[8] Recent studies have shown that PLOD2 is overexpressed in head and neck squamous carcinomas, breast cancer, biliary tract cancer, cervical cancer and colorectal cancer and that it promotes migration, invasion, and proliferation in these tumor cells.[9-13] Previous reports have demonstrated that PLOD2 is regulated by HIF-1α in sarcoma and FOXA1 in non-small-cell lung cancer (NSCLC), which leads to a poor prognosis in these patients.[7,14] In terms of HCC, PLOD2 is associated with the recurrence of early-stage HCC after surgery.[15] However, the potential molecular mechanisms and regulatory signaling pathway by which PLOD2 is involved in the invasion and metastasis process in HCC remain unknown. Hence, identifying the molecular mechanism by which PLOD2 promotes metastasis and invasion in HCC may help us discover potential targets for treatment.

Baculoviral IAP repeat containing 3 (BIRC3), a member of the antiapoptotic protein (IAP) family, has been found to be

Keywords: PLOD2; Hepatocellular carcinoma; Metastasis; Invasion; Proliferation.

Abbreviations: AFP, α-fetoprotein; BCLC, Barcelona Clinic Liver Cancer; BIRC3, Baculoviral IAP repeat containing 3; CI, confidence interval; DMEM, Dulbecco's modified Eagle medium; GSEA, Gene Set Enrichment Analysis; HBsAg, hepatitis B surface antigen; HCC, hepatocellular carcinoma; HR, hazard ratio; IHC, immunohistochemical; IRF5, interferon regulatory factor 5; KD, knockdown; KEGG, Kyoto Encylopaedia of Genes and Genomes; MVI, microvascular invasion; OS, overall survival; NC, Negative control; PLOD2, procollagen-lysine, 2-oxoglutarate 5-dioxygenase 2; RFS, recurrence-free survival; SYSUCC, Sun Yat-sen Cancer Center; TCGA, The Cancer Genome Atlas.

[#]Contributed equally to this work.

[*]**Correspondence to:** Binkui Li and Yunfei Yuan, Department of Liver Surgery, Sun Yat-sen University Cancer Center; 651 Dongfeng Road E. Guangzhou, Guangdong 510060, China. ORCID: https://orcid.org/0000-0003-3201-2914 (BL) and https://orcid.org/0000-0003-2467-3683 (YY). Tel/Fax: +86-20-87343951 (BL) and +86-20-87343118 (YY), E-mail: libk@sysucc.org.cn (BL) and yuanyf@mail.sysu.edu.cn (YY)

highly expressed in a variety of human tumors.[16,17] In addition, BIRC3 regulates the nuclear factor-kappa B (NF-κB) signaling pathway, which is involved in the development of cancers.[18] In this study, we demonstrated that high expression of PLOD2 predicted an unfavorable prognosis in HCC patients, which makes PLOD2 a potential oncogene. Moreover, we verified that PLOD2 promotes HCC invasion and metastasis both *in vitro* and *in vivo*. Mechanistically, we found that inhibition of PLOD2 suppresses HCC cell migration and growth by decreasing BIRC3 expression. Furthermore, we demonstrated that PLOD2 is regulated by interferon regulatory factor 5 (IRF5), which can be responsible for the high expression of PLOD2 in HCC. These data highlighted that PLOD2 plays a critical role in the development of HCC, suggesting that it may serve as a promising novel biomarker for HCC treatment.

Methods

Human tissue specimens and HCC tissue microarray

The HCC and adjacent non-tumor liver tissues prepared into tissue microarray were obtained from 109 patients at the Sun Yat-sen Cancer Center (SYSUCC, Guangzhou, China) between July 2010 and May 2015, and the clinicopathological features are shown in Table 1. The cases selected were based on distinctive pathologic diagnosis of HCC and received curative resection. Average follow-up time was 55.3 months (median: 55.3 months; range: 2.0–105.0 months). Additional HCC tissue from 91 patients received curative resection at SYSUCC were used for immunohistochemical staining study. All samples were obtained with the informed consent of the patients. The study was approved by the Institute Research Ethics Committee at the Cancer Center.

Immunohistochemical (IHC) staining

HCC and adjacent tissues were incubated with anti-PLOD2 antibody (Origene, Rockville, USA), anti-IRF5 (Abcam, Shanghai, China) antibody and anti-BIRC3 antibody (Proteintech, Wuhan, China) respectively at 4°C for 10 h. The details of antibody dilution were shown in Supplementary Table 1. The tissues were then incubated with horseradish peroxidase-conjugated anti-rabbit/mouse antibodies (Dako, Copenhagen, Denmark) at 37°C for 30 m. After that, diaminobenzidine chromogen (Dako) was applied to the samples for reaction followed by counterstaining with hematoxylin (Leagene, Beijing, China). Immunoreactivity for PLOD2, IRF5 and BIRC3 proteins was tested with a semiquantitative method by evaluating the number of positive tumor cells within the total population of tumor cells. Scores were assigned using 5% increments from 0–100% as in our previous study.[19,20] The expression levels of these proteins were divided into four groups based on the IHC scores: negative group, 0–10%; weak group, 11–50%; moderate group, 51–80%; and strong group, 80–100%. We referred to proteins associated with moderate or strong intensities as the high expression group, while proteins associated with tumors of negative or weak intensities were identified as the low expression group.

Cell lines and cell culture

Human HCC cell lines (PLC-8024, Huh7, Hep3B, MHCC-97H and HepG2) and MIHA normal liver cells were purchased from the Shanghai Cell Bank of the Chinese Academy of Sciences (Shanghai, China) with short tandem repeat appraisal certificates. All cells were cultured as described previously.[21] Huh7 and MHCC-97H cells were infected with lentiviral pLKO.1 particles containing short hairpin RNA (shRNA) and were selected with 3 mg/mL puromycin (ThermoFisher, Waltham, MA, USA) for 4 days. Lentiviral pLKO.1 plasmids for shPLOD2 (Jidan, Guangzhou, China) were packaged with Lenti-Pac HIV mix (GeneCopoeia, Guangzhou, China) and Endo-Fectin Lenti (GeneCopoeia, Guangzhou, China) in 293T cells to produce lentiviral particles. For BIRC3 overexpression experiment, the BIRC3 expression plasmid (Jidan, Guangzhou, China) was packaged with Lipofectamine 2000 (ThermoFisher, Waltham, MA, USA) and then infected PLOD2 knockdown (KD) Huh7 and MHCC-97H cells.

Quantitative real-time polymerase chain reaction (qRT-PCR) and western blotting

Total RNA was extracted from cell lines using a TRIzol reagent kit (Life Technologies, Carlsbad, CA, USA). After treatment with DNase I (TaKaRa, Dalian, China), 2 μg of total RNA was used for cDNA synthesis with random hexamers and Superscript III (Invitrogen, Waltham, MA, USA). The primer sequences are shown in Supplementary Table 2. The cDNA templates were subject to PCR amplification. qRT–PCR analysis of PLOD2, IRF5 and BIRC3 was performed on an ABI PRISM 7900 Sequence Detector using SYBR Green PCR Kits (Applied Biosystems, Carlsbad, CA, USA). All reactions were run in triplicate. Cycle threshold values should not differ by more than 0.5 among triplicate reactions. PLOD2, IRF5, and BIRC3 expression levels were normalized to RNU6B, which yielded a $2^{-\Delta\Delta Ct}$ value.

Cell protein lysates were separated on 7.5% sodium dodecyl sulfate-polyacrylamide gels and transferred to polyvinylidene difluoride membranes (Millipore, Burlington, MA, USA), and then incubated with mouse polyclonal antibody specific for PLOD2 (Origene, Rockville, USA), rabbit polyclonal antibody specific for IRF5 (Abcam, Shanghai, China) and rabbit polyclonal antibody specific for BIRC3 (Proteintech, Wuhan, China) at 4°C overnight. Mouse anti-β-actin monoclonal antibody (Sigma–Aldrich, Shanghai, China) was used to estimate protein loading. The details of antibody dilution are shown in Supplementary Table 3.

In vitro cell migration and invasion assays

Cell migration and invasion assays were performed in Transwell chambers (8 μm pore size; CoStar, Washington DC, USA) according to the manufacturer's instructions. Huh7 cells (1.2×10^5) and MHCC-97H cells (2.0×10^5) were placed in the top chamber of each insert (BD Biosciences, Franklin Lakes, NJ, USA) and cultured at 37°C for 24 h. The migrated and invaded cells were stained with crystal violet and photographed at 200× magnification. All measurements were performed in triplicate.

Cell proliferation assay

Cell proliferation was measured using Cell Counting Kit-8 (CCK-8) assay kits (Dojindo Corp., Kumamoto, Japan) according to the manufacturer's instructions. Huh7 cells and MHCC-97H cells (5×10^3) were placed in 96-well plates (1,000 cells per well) and incubated at 37°C for 24 h.

Animal studies

Male BALB/c nude mice at 4 weeks of age were purchased from the Medical Experimental Animal Center of Guangdong Province (China) and fed at the Animal Experimental Center of Sun Yat-Sen University. Experiments involving animals were used randomly. To establish the subcutaneous tumor model, Huh7 cells (4×10^6 cells in 200 μL of serum-free medium) were injected into the right flanks of each group (n=6).

Table 1. Clinical features and PLOD2 protein expression in HCC patients

Characteristics	N	PLOD2 expression		*p*
		High	Low	
Sex				0.750
Male	94	46 (48.94%)	48 (51.06%)	
Female	15	8 (53.33%)	7 (46.67%)	
Age in years				0.640
>50	65	31 (47.69%)	34 (52.31%)	
≤50	44	23 (52.27%)	21 (47.73%)	
BCLC stage				0.030
I	86	38 (44.19%)	48 (55.81%)	
II–III	23	16 (69.57%)	7 (30.43%)	
Histologic grade				<0.001
I–II	57	15 (26.32%)	42 (73.68%)	
III–IV	52	39 (75.00%)	13 (25.00%)	
AFP in μg/L				0.640
≥400	46	24 (52.17%)	22 (47.83%)	
<400	63	30 (47.62%)	33 (52.38%)	
Vascular invasion				0.823
Yes	17	8 (47.06%)	9 (52.94%)	
No	92	46 (50.00%)	46 (50.00%)	
Tumor size in cm				0.001
≤5	54	20 (37.04%)	34 (62.96%)	
>5	55	34 (61.82%)	21 (38.18%)	
Tumor number				0.180
Solitary	94	49 (52.13%)	45 (47.87%)	
Multiple	15	5 (33.33%)	10 (66.67%)	
HBsAg				0.540
Negative	14	8 (57.14%)	6 (42.86%)	
Positive	95	46 (48.42%)	49 (51.58%)	
MVI				0.730
Yes	36	17 (47.22%)	19 (52.78%)	
No	73	37 (50.68%)	36 (49.32%)	
Cirrhosis				0.630
Yes	79	38 (48.10%)	41 (51.90%)	
No	30	16 (53.33%)	14 (46.67%)	
Tumor encapsulation				0.490
Complete	33	18 (54.55%)	15 (45.45%)	
None	76	36 (47.37%)	40 (52.63%)	

AFP, α-fetoprotein; BCLC, Barcelona Clinic Liver Cancer; HBsAg, hepatitis B surface antigen; MVI, microvascular invasion; PLOD2, procollagen-lysine, 2-oxoglutarate 5-dioxygenase 2. $p<0.05$ was considered statistically significant.

Tumor volumes were measured every 3–4 days using a caliper until the day of sacrifice. Tumor volume (V, mm^3) was measured by using the following formula: $V=L\times W^2/2$ where L was the largest diameter in mm, and W the smallest diameter. In the lung metastasis model, Huh7 cells (2×10^6 cells suspended in 200 μL DMEM) were injected through the tail veins ($n=4$). The lungs were dissected after 9 weeks.

Luciferase reporter assay

Luciferase reporter plasmids (full-length and mutant PLOD2 promoters) were constructed by GeneCopoeia (Rockville, IL, USA). Huh7 cells (8.0×10^4) and MHCC-97H cells were seeded

in each well of 24-well plates and incubated at 37°C for 18 h. After that, siIRF5 or negative controls were cotransfected into HCC cells together with PLOD2 promoters. The Secrete-Pair Dual Luminescence Assay Kit (GeneCopoeia, Guangzhou, China) were used to measure the Gaussia luciferase (Gluc) and secreted alkaline phosphatase (SEAP) luciferase activities after 48 h. Gluc activity was normalized to the SEAP activity and each group was analyzed in triplicate experiments.

Cancer genome atlas data analysis

The data for all box plots and correlation plots were retrieved from The Cancer Genome Atlas Data Analysis (https://portal.gdc.cancer.gov/), as RNAseq data in level 3 HTSeq-fragments per kilobase per million (FPKM) format from the liver hepatocellular carcinoma (LIHC) project. Then, the RNAseq data in FPKM were converted into $\log_2$ format. R software (version 3.6.3) was used to create boxplots and correlation plots.

UALCAN analysis

UALCAN (http://ualcan.path.uab.edu) is an interactive web portal for performing in-depth analyses of RNA-seq and clinical data from 31 cancer types of The Cancer Genome Atlas (TCGA) database.[22] In this study, we used UALCAN to analyze the mRNA expression differences in PLOD2 between primary HCC tissues and normal samples. UALCAN was also used to analyze the mRNA expression differences among various subgroups based on cancer stages and tumor grades. Student's *t* test was used to compare the difference in transcriptional expression, and $p<0.05$ was considered statistically significant.

Statistical analysis

The Kaplan–Meier method was used to compute survival curves and survival curves were analyzed by the log-rank test. The multivariate analysis was used to analyze significant prognostic factors found in univariate analysis ($p<0.05$) by the Cox proportional hazards model. Student's *t* test was used to compare any two groups, and one-way analysis of variance was used for multiple comparisons. GraphPad Prism 8.0 software (GraphPad, Inc., La Jolla, CA, USA) and R program (R version 3.6.3; R Foundation for Statistical Computing, Vienna, Austria) were performed for the statistical analysis.

Results

PLOD2 was highly expressed in HCC, and high expression of PLOD2 in HCC predicted poor prognosis

TCGA pan-cancer analysis revealed that PLOD2 was highly expressed in various types of cancers, including kidney renal clear cell carcinoma, lung adenocarcinoma, LIHC and prostate adenocarcinoma compared with expression in normal tissues (Fig. 1A). To investigate the expression of PLOD2 in HCC, we used the TCGA database and found that the mRNA level of PLOD2 was significantly increased in HCC tissues compared with paired adjacent liver tissues (Fig. 1B, C). Moreover, the mRNA expression of PLOD2 was correlated with patients' cancer stages and tumor grades, indicating that higher mRNA expression of PLOD2 was found in advanced cancer stages and increased tumor grades according to the TCGA database (Fig. 1D, E). TCGA database analysis also revealed that higher PLOD2 expression was positively correlated with poor prognosis in human HCC patients (Fig. 1H, I). HCC tissue microarrays including 109 cases of HCC and adjacent liver tissues also demonstrated that PLOD2 protein levels were significantly higher in HCC tissues than adjacent liver tissues (Fig. 1F, G). Additionally, patients with higher PLOD2 expression had shorter overall survival (OS) and recurrence-free survival (RFS) (Fig. 1J and K). Apart from clinical stages and histologic grades, we also found that high PLOD2 expression was significantly associated with tumor size (Table 1). Finally, the analysis of the Cox proportional hazards regression showed that high PLOD2 expression was an independent unfavorable prognostic factor for both OS and RFS (Tables 2 and 3). These results suggest that elevated PLOD2 expression might correlate with aggressive clinicopathological characteristics and poor prognosis in HCC patients.

KD of PLOD2 reduced metastasis and invasion of human HCC cells in vitro and in vivo

We examined the expression of PLOD2 in HCC cell lines and found that PLOD2 was highly expressed in HepG2, Huh7, MHCC-97H and Hep3B cell lines (Fig. 2A). To investigate the functions of PLOD2 in HCC cells, we used shRNA to KD PLOD2 in two HCC cell lines, namely, MHCC-97H and Huh7. Western blotting and qRT-PCR showed that PLOD2 was successfully knocked down by the two shRNAs in both cell lines (Fig. 2B). Transwell and wound healing assays showed that KD of PLOD2 significantly decreased the migration and invasion of HCC cells (Fig. 2C–E). Moreover, KD of PLOD2 slowed down cell growth in both MHCC-97H and Huh7 cells (Fig. 2F).

In addition, we established subcutaneous xenograft and lung metastatic tumor models with Huh7 cells in mice to determine whether PLOD2 deficiency inhibits tumor growth and metastasis *in vivo*. In subcutaneous models, PLOD2 KD reduced the growth of tumors (Fig. 2G), and tumor volume and tumor weight significantly decreased in the PLOD2 KD groups (Fig. 2H, I). Furthermore, the expression of PLOD2 in the KD groups was lower than that in the PLOD2 negative control group (Fig. 2J). The number of Ki-67-positive cells was significantly reduced in cancer tissues with PLOD2 KD (Fig. 2J, K), indicating that the KD of PLOD2 significantly decreased the capacity of tumor growth *in vivo*. Moreover, smaller and fewer metastatic lung nodules were observed in the PLOD2 KD groups than in the control group in our tail vein lung metastasis mouse model (Fig. 2L). Collectively, these results indicate that KD of PLOD2 reduced human HCC cell migration and proliferation.

BIRC3 was the downstream factor of PLOD2 in HCC

To explore the molecular mechanisms by which PLOD2 promotes HCC cell metastasis and invasion, we performed RNA sequencing analysis using the shPLOD2 Huh7 cell line vs. the control, and pathway enrichment was performed via DAVID and gene set enrichment analysis (GSEA). Focal adhesion signaling was one of the most significantly downregulated gene pathways that resulted from PLOD2 KD (Fig. 3A). GSEA revealed that focal adhesion signaling was prominently inhibited in HCC with the KD of PLOD2 (Fig. 3B). Focal adhesion signaling is a pathway that interacts with cells and extracellular matrix which plays essential roles in biological processes, including cell motility, cell proliferation, cell differentiation, regulation of gene expression and cell survival. Moreover, previous study showed that PLOD2 promoted the migration and invasion of cervical cancer cells by focal adhesion formation.[12,23] Because PLOD2 is an oncogene related to extracellular matrix, we hypothesized that KD of PLOD2 inhibits HCC cell proliferation by inhibiting the focal adhesion signaling pathway. We used real-time polymerase chain reaction assays to confirm that PLOD2 KD decreased the mRNA expression of genes of the focal adhesion signaling pathway, including COMP, CAV1, CAV2, EGF, BIRC3 and CAPN2 (Fig. 3C).

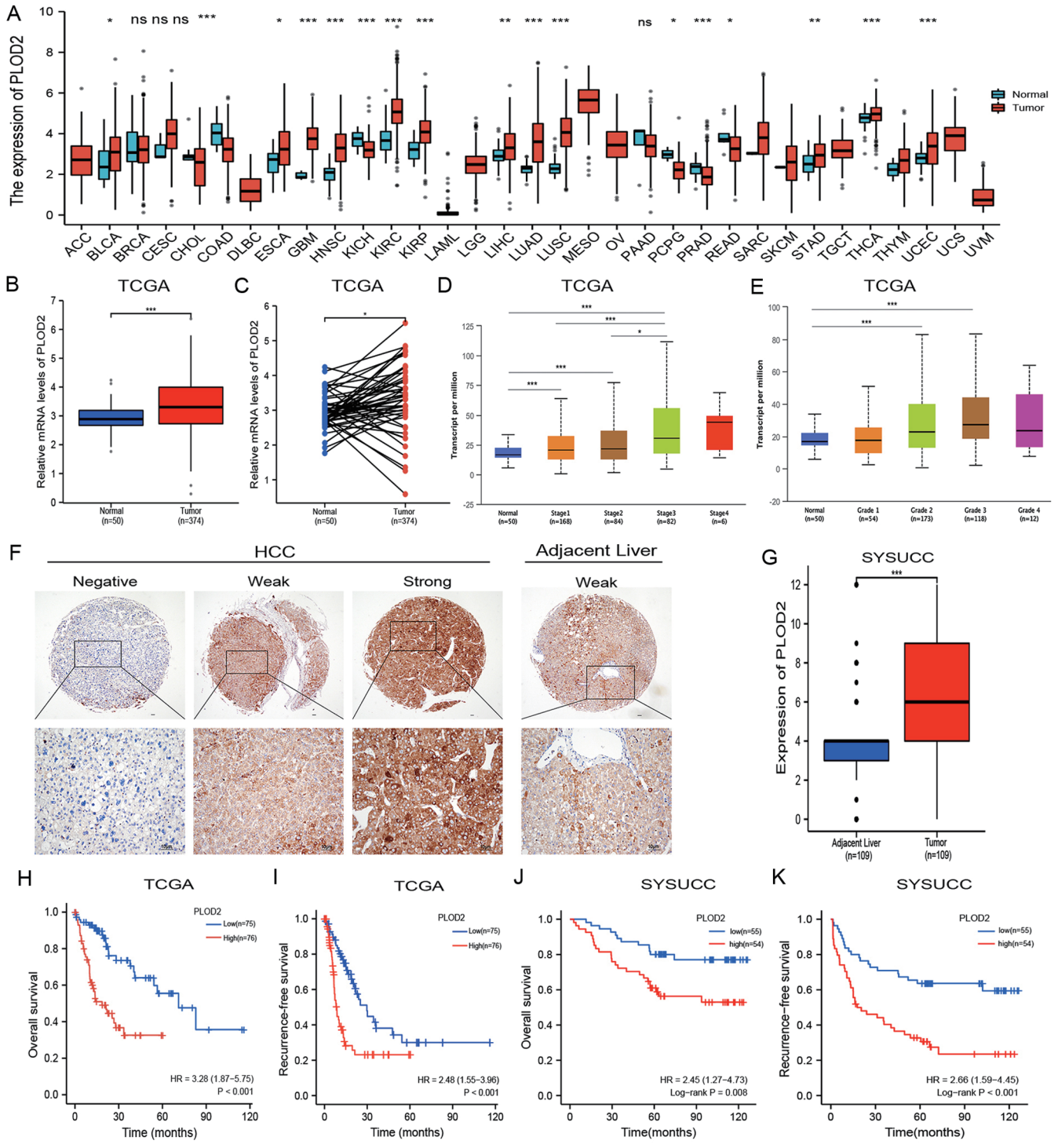

Fig. 1. PLOD2 was upregulated and correlated with poor prognosis in HCC. (A) Pan-cancer analysis of PLOD2 expression in different tumor types from The Cancer Genome Atlas (TCGA) database. (B) Relative mRNA levels of PLOD2 in HCC and normal tissues were determined based on the TCGA dataset. $^{**}p<0.001$. (C) Relative mRNA levels of PLOD2 were significantly increased in HCC tissues compared with adjacent normal tissues based on the TCGA dataset. $^{*}p<0.05$. (D) mRNA expression of PLOD2 was significantly correlated with HCC patients' individual cancer stages. $^{*}p<0.05$, $^{***}p<0.00$. (E) mRNA expression of PLOD2 was positively correlated with tumor histologic grades of HCC. $^{*}p<0.05$, $^{***}p<0.001$. (F, G) Representative IHC staining images showed that PLOD2 expression was significantly increased in HCC tissues based on the SYSUCC dataset (left). Protein level of PLOD2 were significantly increased in HCC tissues compared with paired adjacent liver tissues based on the SYSUCC dataset (Right). $^{***}p<0.001$. (H–I) PLOD2 mRNA expression was correlated with shorter overall and recurrence-free survival times in HCC patients based on the TCGA dataset; (J–K) Kaplan–Meier plots revealed that shorter overall and recurrence-free survival times were correlated with higher PLOD2 expression in the SYSUCC validation cohort. HCC, hepatocellular carcinoma; IHC, immunohistochemical; PLOD2, procollagen-lysine, 2-oxoglutarate 5-dioxygenase 2; SYSUCC, Sun Yat-sen Cancer Center; TCGA, The Cancer Genome Atlas.

Table 2. Univariate and multivariate Cox regression analyses for overall survival

Variable	Univariate analysis		Multivariate analysis	
	HR (95% CI)	*p*	HR (95% CI)	*p*
PLOD2, high vs. low	2.47 (1.24–4.95)	0.011	2.12 (1.01–4.46)	0.046
Sex, M vs. F	5.62 (0.77–41.01)	0.089		
Age, ≥50 vs. 50 years	0.64 (0.33–1.23)	0.180		
BCLC stage, I vs. II–III	4.27 (2.22–8.24)	<0.001	2.51 (1.11–5.68)	0.028
Histologic grade, I–II vs. III–IV	1.53 (0.79–2.54)	0.206		
HBsAg, positive vs. negative	0.72 (0.30–1.73)	0.721		
Cirrhosis, yes vs. no	1.34 (0.66–2.76)	0.422		
MVI, present vs. absent	1.75 (0.89–3.42)	0.103		
Tumor capsule, none vs. complete	1.26 (0.63–2.52)	0.514		
Tumor size, ≥5 cm vs. <5 cm	2.24 (1.12–4.48)	0.023		
Tumor number, multiple vs. solitary	1.31(0.31–5.47)	0.712		
AFP, ≥400 vs. <400 μg/L	1.22 (0.63–2.37)	0.55		
Vascular invasion, present vs. absent	2.99 (1.53–5.85)	0.001		

AFP, α-fetoprotein; BCLC, Barcelona Clinic Liver Cancer; CI, confidence interval; MVI, microvascular invasion; HBsAg, hepatitis B surface antigen; HR, hazard ratio; PLOD2, procollagen-lysine, 2-oxoglutarate 5-dioxygenase 2. $p<0.05$ was considered statistically significant.

Focal adhesion signaling receptor BIRC3 is an oncogene that promotes cell invasion and proliferation via NF-κB signaling in HCC.[24,25] Moreover, BIRC3 is regulated by COL11A1 and enhances ovarian cancer cell resistance to cisplatin thereby promoting ovarian cancer progression.[26] Given that BIRC3 is an oncogene that related to collagen, we hypothesized that PLOD2 promotes HCC cell migration and proliferation via BIRC3. To verify the hypothesis, we performed western blotting to demonstrate that the expression of BIRC3 was decreased by KD of PLOD2 in HCC cells (Fig. 3D). To test the relationship between PLOD2 and BIRC3, we examined the protein levels of PLOD2 and BIRC3 in a total of 200 HCC specimens using tissue microarrays by IHC (Fig. 3E). The expression of BIRC3 was significantly correlated with the levels of PLOD2 in human HCC specimens (Fig. 3F). We further analyzed the TCGA database and found that the relationship between BIRC3 and PLOD2 mRNA levels was positively correlated (Fig. 3G), which was consistent with our results. Taken together, our data illustrated that the expression of BIRC3 was the downstream factor of PLOD2 in HCC.

KD of PLOD2 inhibited HCC cell metastasis and invasion by decreasing BIRC3 expression

Given that BIRC3 is regulated by PLOD2, we focused on whether loss of PLOD2 inhibits HCC metastasis and invasion by decreasing BIRC3 expression. We first overexpressed

Table 3. Univariate and multivariate Cox regression analyses for recurrence-free survival

Variable	Univariate analysis		Multivariate analysis	
	HR (95% CI)	*p*	HR (95% CI)	*p*
PLOD2, high vs. low	2.73 (1.60–4.66)	<0.001	2.43 (1.29–4.56)	0.006
Sex, M vs. F	1.65 (0.71–3.83)	0.247		
Age, ≥50 vs. <50 years	0.74 (0.45–1.24)	0.255		
BCLC stage, I vs. II–III	2.88 (1.69–4.91)	<0.001	1.93 (1.00–3.73)	0.049
Histologic grade, I–II vs. III–IV	1.68 (1.00–2.79)	0.046		
HBsAg, positive vs. negative	1.54 (0.66–3.58)	0.318		
Cirrhosis, yes vs. no	1.00 (0.59–1.69)	0.994		
MVI, present vs. absent	1.59 (0.93–2.71)	0.087		
Tumor capsule, none vs. complete	0.912 (0.54–1.53)	0.726		
Tumor size, ≥5 cm vs. <5 cm	2.04 (1.21–3.44)	0.007		
Tumor number, multiple vs. solitary	1.06 (0.33–3.40)	0.918		
AFP, ≥400 vs. <400 μg/L	1.49 (0.89–2.48)	0.127		
Vascular invasion, present vs. absent	1.80 (1.01–3.20)	0.045		

AFP, α-fetoprotein; BCLC, Barcelona Clinic Liver Cancer; CI, confidence interval; MVI, microvascular invasion; HBsAg, hepatitis B surface antigen; HR, hazard ratio; PLOD2, procollagen-lysine, 2-oxoglutarate 5-dioxygenase 2. $p<0.05$ was considered statistically significant.

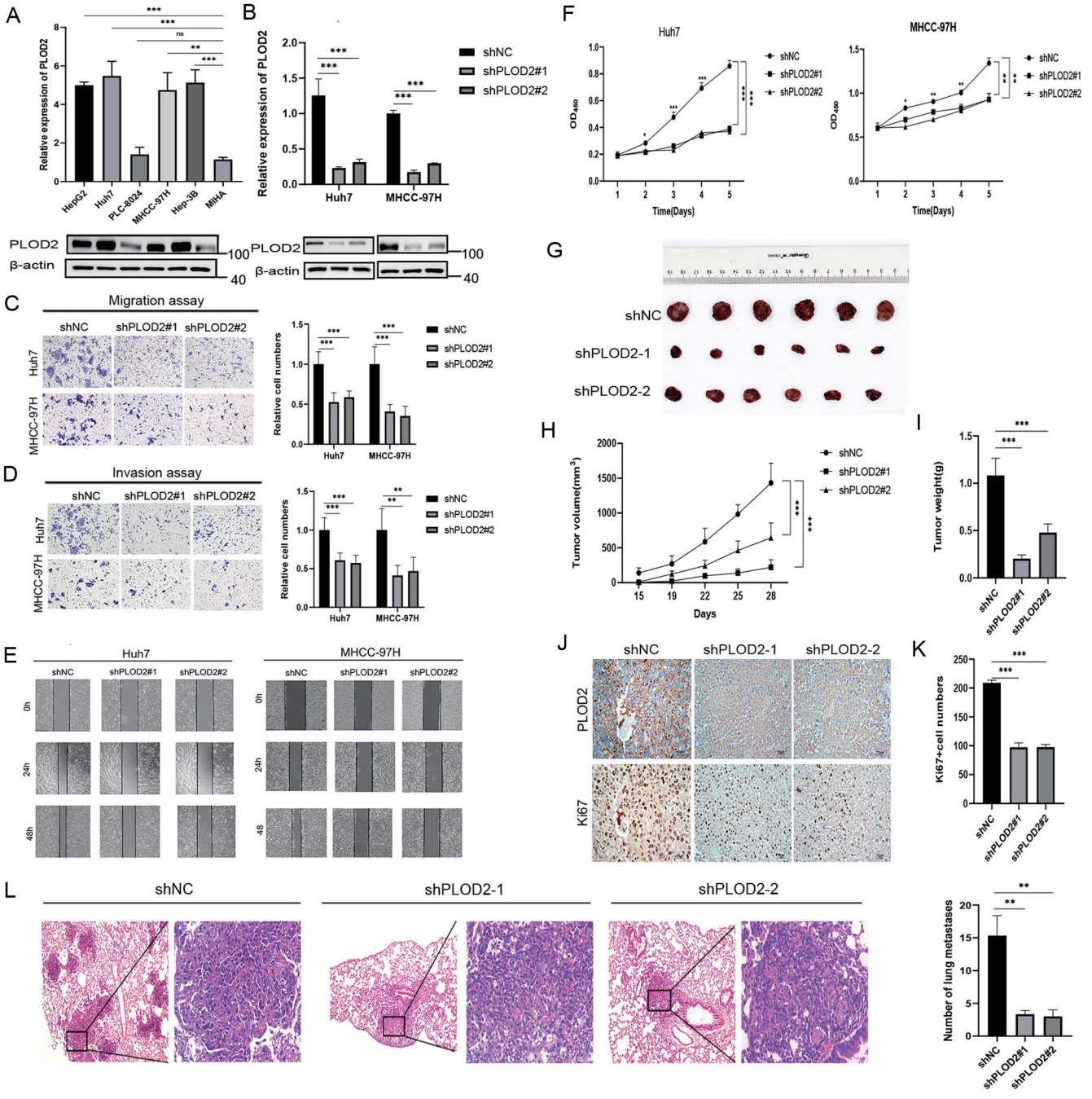

Fig. 2. KD of PLOD2 decreased the metastasis and invasion of HCC cells *in vitro* and *in vivo*. (A) qPCR (top) and western blot (bottom) showing the expression of PLOD2 in MIHA and 5 HCC cell lines. (B) The efficiency of PLOD2 KD was measured by real-time PCR (top) and western blotting (bottom) assays. ***p<0.001. (C) KD of PLOD2 decreased Huh7 and MHCC-97H cell migration. ***p<0.001. (D) KD of PLOD2 decreased Huh7 and MHCC-97H cell invasion. **p<0.01, ***p<0.001. (E) KD of PLOD2 impaired the scratch wound healing ability of Huh7 and MHCC-97H cells. (F) KD of PLOD2 inhibited Huh7 and MHCC-97H cell proliferation. **p<0.01, ***p<0.001. (G, H) KD of PLOD2 significantly inhibited tumor size and growth. ***p<0.001. (I) KD of PLOD2 significantly inhibited tumor weight. ***p<0.001. (J) Representative IHC staining images showing that the expression of PLOD2 and Ki67 were significantly decreased in the KD groups. (K) KD of PLOD2 significantly suppressed the expression of Ki67 in a nude mouse model established by injection of Huh7 cells into the right flank (n=6). ***p<0.001. (L) KD of PLOD2 significantly suppressed lung metastasis in a nude mouse model established by injection of Huh7 cells through the tail vein (n=4). **p<0.01. HCC, hepatocellular carcinoma; IHC, immunohistochemical; KD, knockdown; PLOD2, procollagen-lysine, 2-oxoglutarate 5-dioxygenase 2.

BIRC3 in PLOD2 KD Huh7 and MHCC-97H cell lines (Fig. 4A). Overexpression of BIRC3 promoted cell proliferation, migration, and invasion, which rescued the phenotype caused by PLOD2 KD in HCC cells (Fig. 4B–D). Moreover, overexpression of BIRC3 promoted cell migration and restored the decreased wound healing ability caused by PLOD2 KD in HCC cells (Fig. 4E). In subcutaneous models, the expression of BIRC3 was reduced in the KD groups compared with the

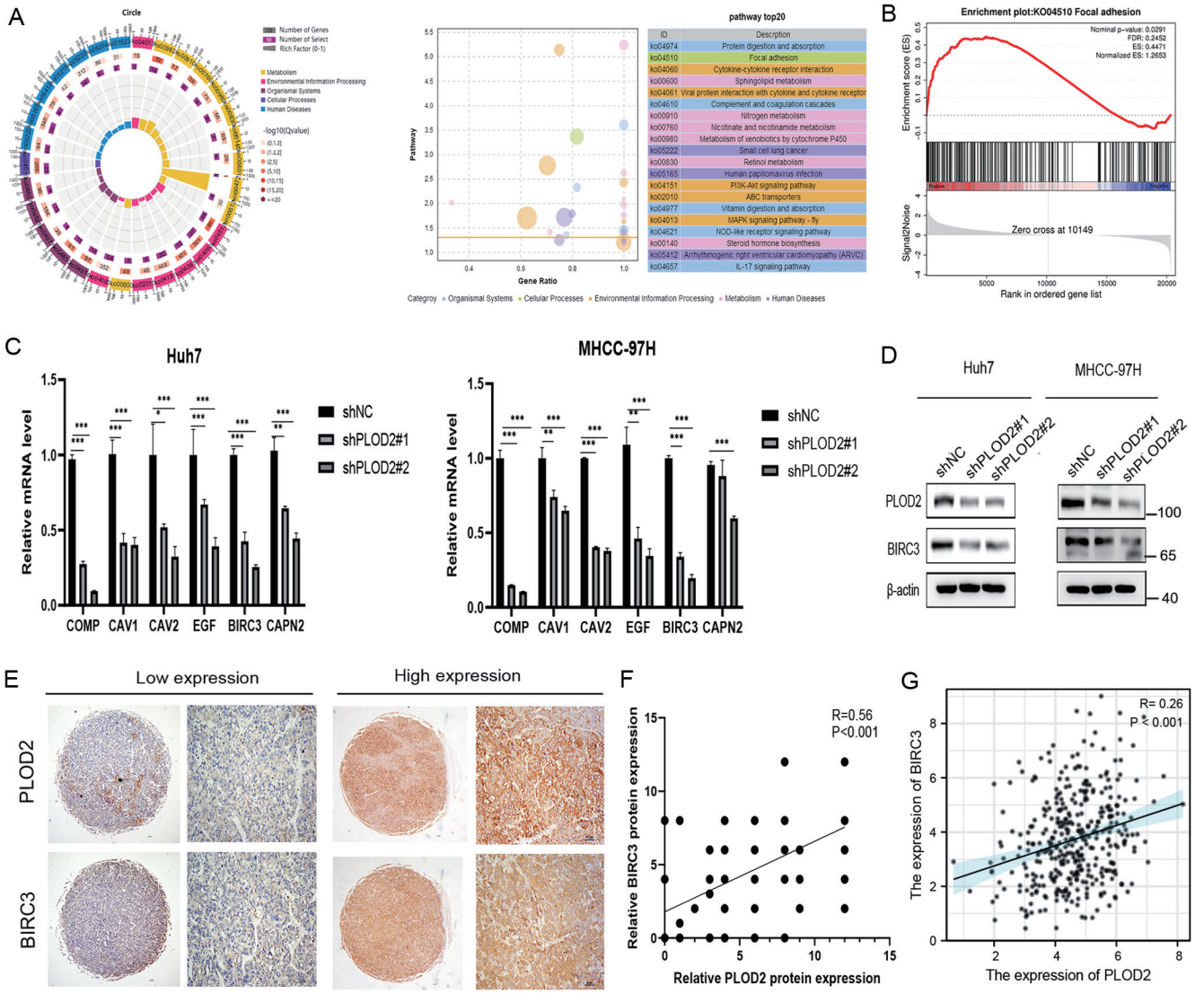

Fig. 3. BIRC3 was regulated by PLOD2 in HCC. (A) KEGG pathway analysis shows the significantly affected signaling pathways in Huh7 cells. (B) GSEA showing the enrichment of Focal adhesion-related gene signatures in PLOD2 KD cells. (C) Relative mRNA levels of genes in the Focal adhesion signaling pathway in Huh7 and MHCC-97H cells. *$p<0.05$, ***$p<0.001$. (D) Western blot assays showing the relative levels of PLOD2 and BIRC3 after PLOD2 KD in Huh7 and MHCC-97H cells. (E, F) Representative IHC staining images show a positive correlation between PLOD2 and BIRC3 levels in human HCC samples (n=200). (G) Correlation of PLOD2 and BIRC3 mRNAs in HCC samples from the TCGA database. BIRC3, Baculoviral IAP repeat containing 3; GSEA, Gene Set Enrichment Analysis; HCC, hepatocellular carcinoma; KD, knockdown; KEGG, Kyoto Encyclopaedia of Genes and Genomes; PLOD2, procollagen-lysine, 2-oxoglutarate 5-dioxygenase 2; TCGA, The Cancer Genome Atlas.

negative control group (Fig. 4F–G), indicating that BIRC3 is regulated by PLOD2 *in vivo*. Overall, our results demonstrate that KD of PLOD2 inhibited HCC cell migration and growth by decreasing BIRC3 expression.

PLOD2 transcription was regulated by IRF5

According to previous reports, the differential expression of PLOD2 is regulated at the transcriptional level in multiple human carcinomas.[7,14] Thus, we analyzed the promoter region of PLOD2 (+99 to −2,000 kb) in JASPAR (http://jaspar.genereg.net/). Using 10 scores as a cutoff point and 80% as the relative profile score threshold, four potential genes were selected as the underlying transcription factors. Interferon regulatory factor 5 (IRF5) is a transcription factor with diverse functions, including modulation of cell growth, differentiation, apoptosis, and immune system activity. Moreover, the mRNA level of IRF5 was higher in HCC tissues than in normal tissues and correlated with poor prognosis according to TCGA analysis (Fig. 5A, B). We therefore hypothesized that PLOD2 is regulated by IRF5 at the transcriptional level. To verify our hypothesis, we silenced IRF5 with siRNA in the Huh7 and MHCC-97H cell lines. The mRNA and protein expression levels of PLOD2 were significantly decreased after specifically silencing IRF5 (Fig. 5C, D). In addition, IHC of tissue microarray including 200 HCC samples indicated that PLOD2 was positively correlated with IRF5 at the protein level (Fig. 5E), consistent with the mRNA level confirmed by TCGA database analysis (Fig. 5F). According to the JASPAR results, two binding sites of IRF5 were predicted in the putative promoter region of PLOD2 (Fig. 5G). To further explore the binding site, we performed a promoter activity assay using a plasmid constructed by linking the PLOD2 promoter to

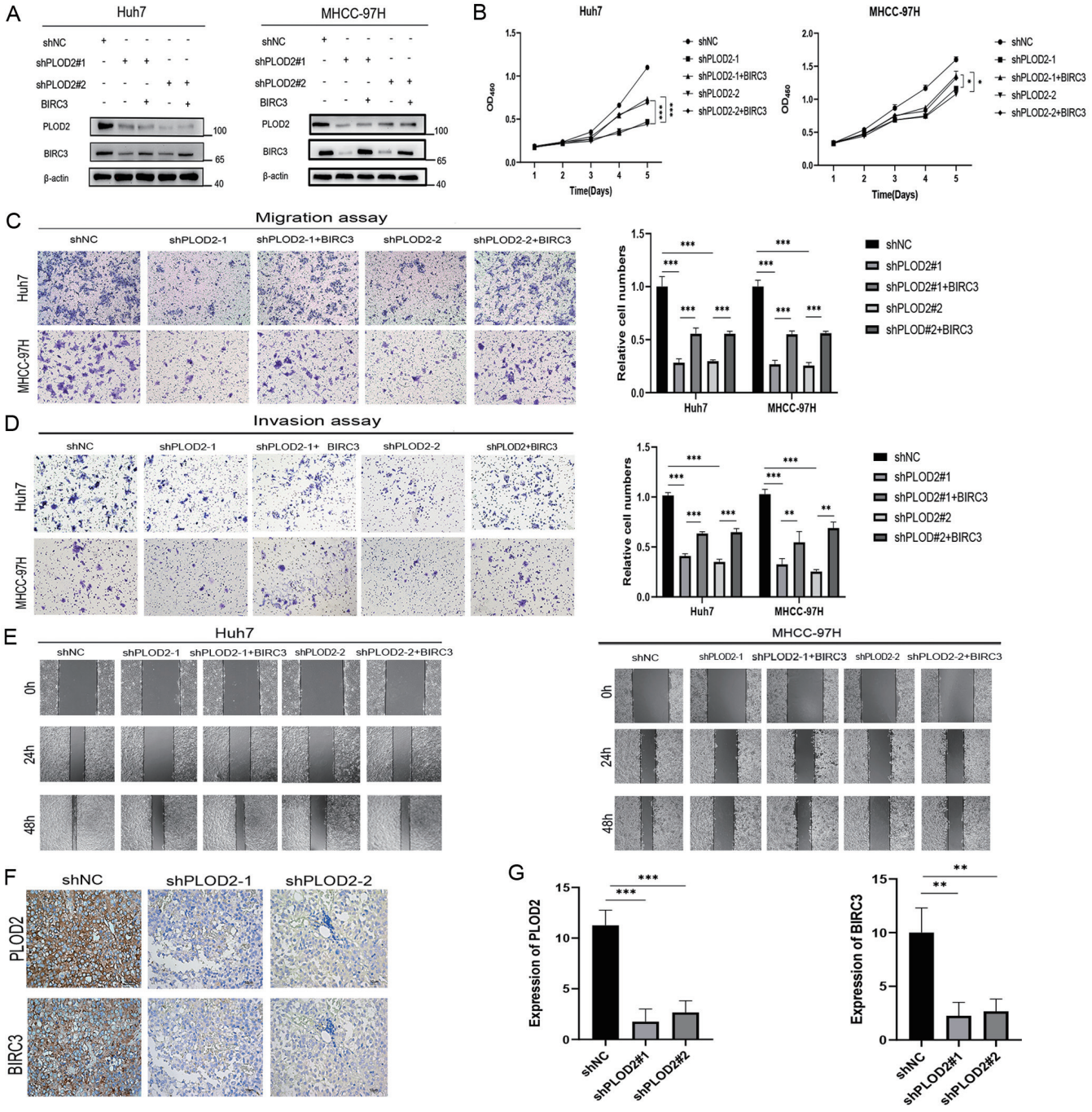

Fig. 4. KD of PLOD2 inhibited HCC cell migration, invasion, and proliferation by decreasing BIRC3 expression. (A) Western blots show relative levels of PLOD2 and BIRC3 after BIRC3 overexpression in PLOD2 KD HCC cells. (B) CCK-8 assays demonstrated that overexpression of BIRC3 increased cell proliferation in PLOD2 KD HCC cells. *p<0.05, ***p<0.001. (C) Transwell assays demonstrated that overexpression of BIRC3 increased cell migration in PLOD2 KD HCC cells. ***p<0.001. (D) Transwell assays demonstrated that overexpression of BIRC3 increased cell invasion in PLOD2 KD HCC cells. **p<0.01, ***p<0.001. (E) Wound healing assays demonstrated that overexpression of BIRC3 increased cell migration in PLOD2 KD HCC cells. (F–G) KD of PLOD2 significantly suppressed the expression of PLOD2 and BIRC3 in a nude mouse model established by injection of Huh7 cells into the right flank (n=6). **p<0.01, ***p<0.001. BIRC3, Baculoviral IAP repeat containing 3; HCC, hepatocellular carcinoma; KD, knockdown; PLOD2, procollagen-lysine, 2-oxoglutarate 5-dioxygenase 2.

a luciferase gene. Promoter luciferase assays showed that the transcriptional activity of the full-length PLOD2 promoter was significantly reduced when IRF5 was silenced with siRNA (Fig. 5H). Next, we identified the functional IRF5 binding region in the PLOD2 promoter by mutating two potential binding regions (Fig. 5J, K). IRF5 silencing significantly reduced the luciferase activity of mutant site A, while the luciferase activity of mutant site B construct remained similar to that of the control group (Fig. 5I–L). The results show that site B was the binding site of IRF5, regulated the transcription and

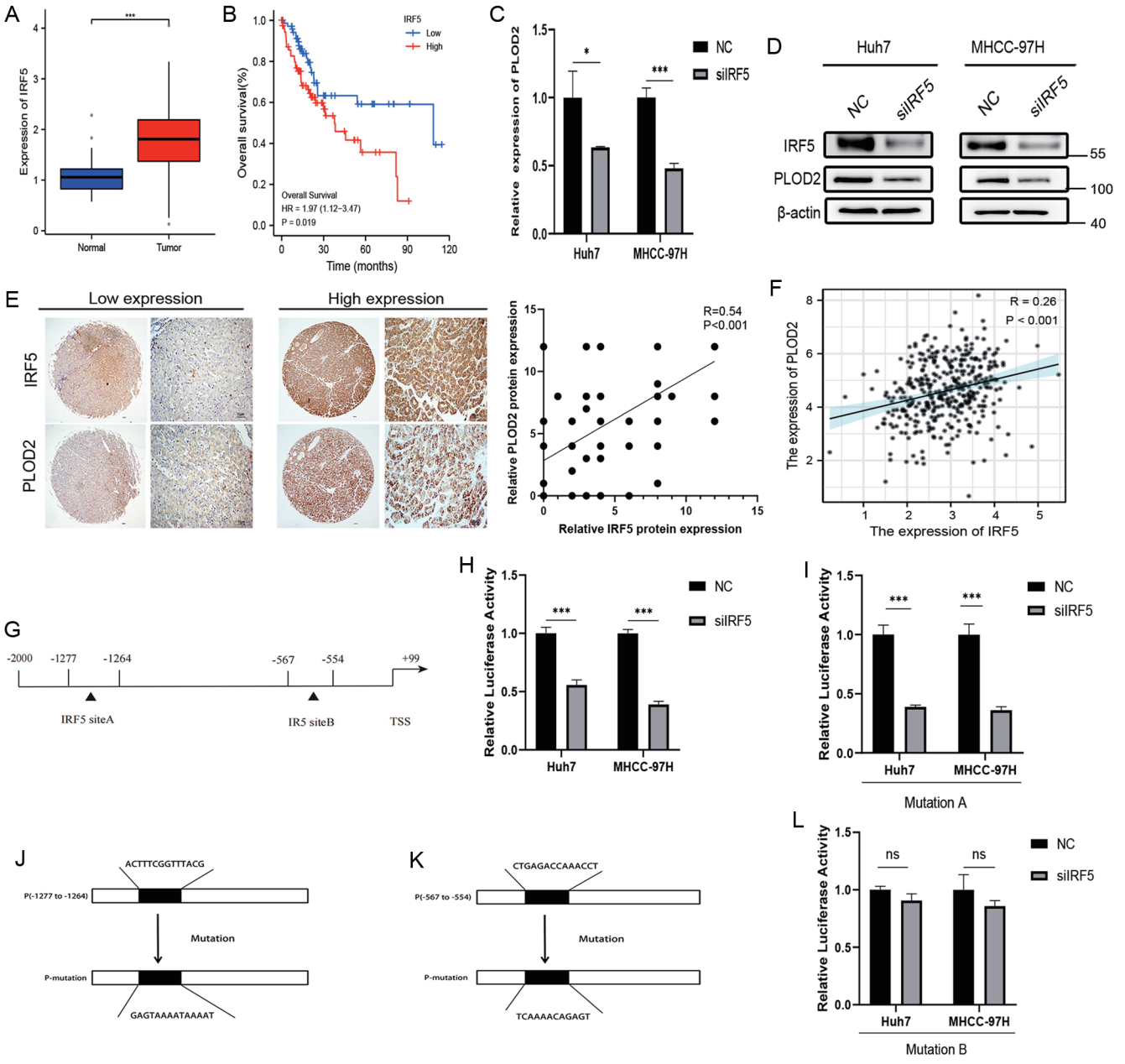

Fig. 5. IRF5 regulated PLOD2 expression by activating the PLOD2 promoter. (A) Relative mRNA levels of PLOD2 in HCC and normal tissues were determined based on the TCGA dataset. ***p<0.001. (B) IRF5 mRNA expression was correlated with poor survival in HCC patients based on the TCGA dataset. (C, D) qPCR and western blot assays showing the relative levels of IRF5 and PLOD2 in the siIRF5 Huh7 and MHCC-97H cell lines. *p<0.05, ***p<0.001. (E) Representative IHC staining images showing a positive correlation between IRF5 and PLOD2 levels in human HCC samples (n=200). (F) Correlation of IRF5 and PLOD2 mRNAs in HCC samples from the TCGA database. (G) Schematic view of the luciferase reporter constructs containing various sites of PLOD2. (H) KD of IRF5 reduced PLOD2 promoter activity. HCC cells were reversely transfected with NC or siIRF5 for 24 h, followed by transfection with the full-length PLOD2 promoter (−2,000/+99) for another 48 h, and then were subjected to luciferase activity assay. ***p<0.001. (I) KD of IRF5 decreased the luciferase activity of the site A mutant. HCC cells were reversely transfected with NC or siIRF5 for 24 h, followed by transfection with the site A mutant for another 48 h and then were subjected to luciferase activity assay. ***p<0.001. (J) The sequence of site A and the corresponding sequence of the mutated site are shown. (K) The sequence of site B and the corresponding sequence of the mutated site are shown. (L) KD of IRF5 did not change the luciferase activity of the site B mutant. HCC cells were reversely transfected with NC or siIRF5 for 24 h, followed by transfection with the site B mutant for another 48 h, and then were subjected to luciferase activity assay. HCC, hepatocellular carcinoma; IHC, immunohistochemical; IRF5, interferon regulatory factor 5; KD, knockdown; NC, Negative control; PLOD2, procollagen-lysine, 2-oxoglutarate 5-dioxygenase 2; TCGA, The Cancer Genome Atlas.

PLOD2 expression in HCC cells.

Altogether, our results suggest that PLOD2 acts as a tumor promoter regulated by IRF5 and promotes progression of HCC via BIRC3, providing a molecular mechanism for the increased aggressiveness in PLOD2 highly expressed tumors (Fig. 6).

Discussion

The poor behaviors of HCC may be attributed to tumor me-

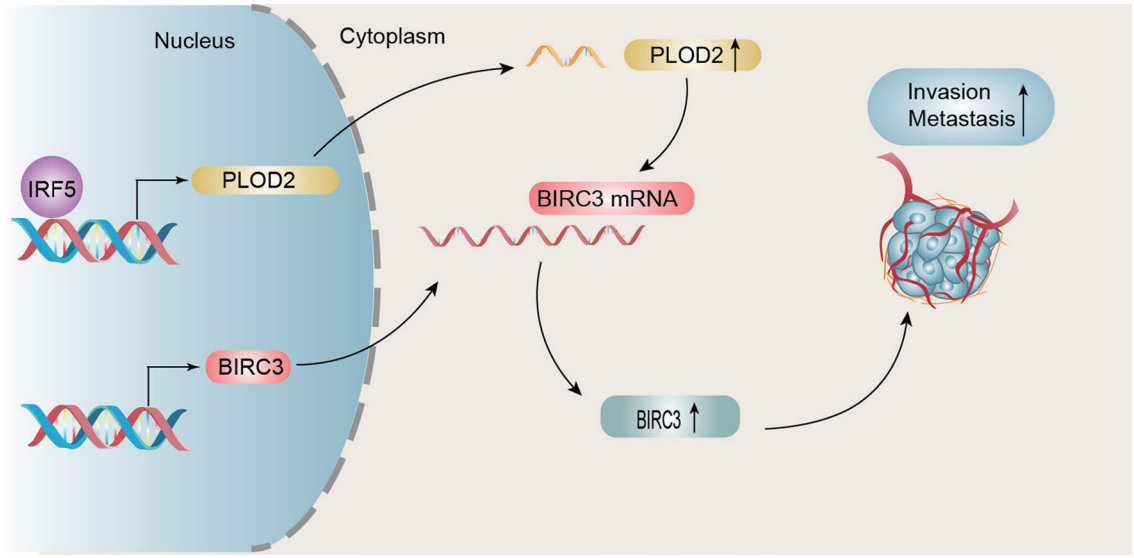

Fig. 6. Schematic regulatory network showing that upregulation of PLOD2 promotes metastasis in HCC. HCC, hepatocellular carcinoma; PLOD2, procollagen-lysine, 2-oxoglutarate 5-dioxygenase 2.

tastasis and invasion. In multiple cancers, these aggressive behaviors may be attributed to accumulated collagen deposition and cross-linking, which lead to poor prognosis in tumor patients.[27-30] Tougher tumor stroma was generated by cross-linking via PLOD2-dependent collagen modification and organization,7 which could be regarded as an 'expressway' for tumor cells migrating to remote organs and blood vessels in tumor patients, resulting in metastasis. These reports have revealed the relationship between PLOD2 and the degree of malignancy, indicating that PLOD2 might be a potential molecular marker for several cancers. In this study, we found that increased PLOD2 expression in HCC tissues is correlated with poor prognosis in HCC patients. Moreover, the expression of PLOD2 was related to HCC tumor size, grade, and cancer BCLC stage. Furthermore, PLOD2 could be regarded as an independent unfavorable prognostic factor for both OS and RFS in HCC patients. By *in vitro* and *in vivo* experiments, we confirmed that KD of PLOD2 inhibits HCC cell metastasis and invasion, suggesting that PLOD2 may be a promising oncogene for HCC.

Based on the results, we explored the potential molecular mechanism by which PLOD2 promotes HCC development. However, the signaling pathways and target genes regulated by PLOD2 have not been discovered. In our study, RNA sequencing revealed that PLOD2 participates in the focal adhesion signaling pathway. Due to the high expression of BIRC3 found in a variety of human malignant tumors and BIRC3 involved in multiple biological processes, including cell proliferation, migration and apoptosis,[18,31,32] we selected BIRC3 as the target gene of PLOD2 among various alternative genes. Furthermore, we demonstrated that HCC cells promoted metastasis and invasion via PLOD2-mediated activation of BIRC3. In summary, our study first discovered the target gene regulated by PLOD2.

PLOD2 has been reported to be regulated at the transcriptional level by numerous transcription factors, such as FOXA1, HIF-1α and TGFβ1, in multiple tumors.[7,14,33] Interferon regulatory factor 5 (IRF5) is a member of the IRF family and plays a critical role in diverse immunomodulatory activities.[34] In our study, we not only found that IRF5 and PLOD2 are positively correlated but also demonstrated that IRF5 can bind to the promoter of PLOD2 and regulate the expression of PLOD2 in HCC. Although IRF5 is expressed at low levels in a variety of tumors and is positively correlated with the prognosis of these tumors, we demonstrated that IRF5 is overexpressed in HCC tissue and correlated with poor prognosis in HCC patients. These results clarified that IRF5 could transcriptionally regulate the expression of PLOD2 and explained why PLOD2 is upregulated in HCC tissues.

In addition to these results, there are some limitations in this study. First, the detailed molecular interaction mechanism between PLOD2 and BIRC3 in HCC has not been elucidated. Moreover, due to technical limitations, we failed to perform a chromatin immunoprecipitation assay to prove that PLOD2 is directly regulated by IRF5. In addition, we need to perform rescue experiments *in vivo* to verify that PLOD2 promotes HCC cell metastasis and invasion via BIRC3.

Conclusions

In summary, our present work identified that PLOD2 plays a critical role in HCC invasion and metastasis by activating BIRC3. KD of PLOD2 significantly suppresses the malignant phenotype of HCC. Thus, our findings provide valuable evidence that PLOD2 may be a prognostic biomarker and a novel therapeutic target for HCC treatment.

Acknowledgments

The authors would like to thank all the members who made contributions to this research.

Funding

This work was supported by grants from the National Natural Science Foundation of China (Nos. 81902473, 82172815, and 82103601).

Conflict of interest

The authors have no conflict of interests related to this publication.

Author contributions

Study conception and design (KrL, YN, KL, CZ, ZQ, YhY, YS, ZL, ZH, DZ, YfY, BL), performance of experiments, analysis of the data and writing of the manuscript (KrL, YN), collection of the clinical samples (CZ, ZQ), assistance with the immunohistochemistry assays and animal experiments (YhY, YS, ZL, ZH, DZ), and revision of the manuscript (YfY, BL). All authors read and approved the final manuscript.

Ethical statement

The Institutional Review Board of Sun Yat-Sen University Cancer Center approved this study (B2022-095-01). The Institutional Animal Care and Use Committee of Sun Yat-Sen University Cancer Center approved this study. The Laboratory Animal-Guideline for ethical review of animal welfare (GB/T 35892-2018) were adhered to regarding the use of animals in this research.

Data sharing statement

All data generated or analyzed during this study are included in this article.

References

[1] Bray F, Ferlay J, Soerjomataram I, Siegel RL, Torre LA, Jemal A. Global cancer statistics 2018: GLOBOCAN estimates of incidence and mortality worldwide for 36 cancers in 185 countries. CA Cancer J Clin 2018;68(6):394–424. doi:10.3322/caac.21492, PMID:30207593.

[2] Zeng H, Chen W, Zheng R, Zhang S, Ji JS, Zou X, *et al*. Changing cancer survival in China during 2003-15: a pooled analysis of 17 population-based cancer registries. Lancet Glob Health 2018;6(5):e555–e567. doi:10.1016/S2214-109X(18)30127-X, PMID:29653628.

[3] Siegel RL, Miller KD, Fuchs HE, Jemal A. Cancer Statistics, 2021. CA Cancer J Clin 2021;71(1):7–33. doi:10.3322/caac.21654, PMID:33433946.

[4] Xiong G, Deng L, Zhu J, Rychahou PG, Xu R. Prolyl-4-hydroxylase α subunit 2 promotes breast cancer progression and metastasis by regulating collagen deposition. BMC Cancer 2014;14:1. doi:10.1186/1471-2407-14-1, PMID:24383403.

[5] Pollard JW. Tumour-educated macrophages promote tumour progression and metastasis. Nat Rev Cancer 2004;4(1):71–78. doi:10.1038/nrc1256, PMID:14708027.

[6] Cheon DJ, Tong Y, Sim MS, Dering J, Berel D, Cui X, *et al*. A collagen-remodeling gene signature regulated by TGF-β signaling is associated with metastasis and poor survival in serous ovarian cancer. Clin Cancer Res 2014;20(3):711–723. doi:10.1158/1078-0432.Ccr-13-1256, PMID:24218511.

[7] Eisinger-Mathason TS, Zhang M, Qiu Q, Skuli N, Nakazawa MS, Karakasheva T, *et al*. Hypoxia-dependent modification of collagen networks promotes sarcoma metastasis. Cancer Discov 2013;3(10):1190–1205. doi:10.1158/2159-8290.Cd-13-0118, PMID:23906982.

[8] Chen Y, Terajima M, Yang Y, Sun L, Ahn YH, Pankova D, *et al*. Lysyl hydroxylase 2 induces a collagen cross-link switch in tumor stroma. J Clin Invest 2015;125(3):1147–1162. doi:10.1172/jci74725, PMID:25664850.

[9] Sato K, Parag-Sharma K, Terajima M, Musicant AM, Murphy RM, Ramsey MR, *et al*. Lysyl hydroxylase 2-induced collagen cross-link switching promotes metastasis in head and neck squamous cell carcinomas. Neoplasia 2021;23(6):594–606. doi:10.1016/j.neo.2021.05.014, PMID:34107376.

[10] He JY, Wei XH, Li SJ, Liu Y, Hu HL, Li ZZ, *et al*. Adipocyte-derived IL-6 and leptin promote breast Cancer metastasis via upregulation of Lysyl Hydroxylase-2 expression. Cell Commun Signal 2018;16(1):100. doi:10.1186/s12964-018-0309-z, PMID:30563531.

[11] Okumura Y, Noda T, Eguchi H, Sakamoto T, Iwagami Y, Yamada D, *et al*. Hypoxia-Induced PLOD2 is a Key Regulator in Epithelial-Mesenchymal Transition and Chemoresistance in Biliary Tract Cancer. Ann Surg Oncol 2018;25(12):3728–3737. doi:10.1245/s10434-018-6670-8, PMID:30105440.

[12] Xu F, Zhang J, Hu G, Liu L, Liang W. Hypoxia and TGF-β1 induced PLOD2 expression improve the migration and invasion of cervical cancer cells by promoting epithelial-to-mesenchymal transition (EMT) and focal adhesion formation. Cancer Cell Int 2017;17:54. doi:10.1186/s12935-017-0420-z, PMID:28507454.

[13] Shao Y, Xu K, Zheng X, Zhou B, Zhang X, Wang L, *et al*. Proteomics profiling of colorectal cancer progression identifies PLOD2 as a potential therapeutic target. Cancer Commun (Lond) 2022;42(2):164–169. doi:10.1002/cac2.12240, PMID:34862750.

[14] Du H, Chen Y, Hou X, Huang Y, Wei X, Yu X, *et al*. PLOD2 regulated by transcription factor FOXA1 promotes metastasis in NSCLC. Cell Death Dis 2017;8(10):e3143. doi:10.1038/cddis.2017.553, PMID:29072684.

[15] Noda T, Yamamoto H, Takemasa I, Yamada D, Uemura M, Wada H, *et al*. PLOD2 induced under hypoxia is a novel prognostic factor for hepatocellular carcinoma after curative resection. Liver Int 2012;32(1):110–118. doi:10.1111/j.1478-3231.2011.02619.x, PMID:22098155.

[16] Ivagnès A, Messaoudene M, Stoll G, Routy B, Fluckiger A, Yamazaki T, *et al*. TNFR2/BIRC3-TRAF1 signaling pathway as a novel NK cell immune checkpoint in cancer. Oncoimmunology 2018;7(12):e1386826. doi:10.1080/2162402x.2017.1386826, PMID:30524877.

[17] Yang C, Wang H, Zhang B, Chen Y, Zhang Y, Sun X, *et al*. LCL161 increases paclitaxel-induced apoptosis by degrading cIAP1 and cIAP2 in NSCLC. J Exp Clin Cancer Res 2016;35(1):158. doi:10.1186/s13046-016-0435-7, PMID:27737687.

[18] Jiang X, Li C, Lin B, Hong H, Jiang L, Zhu S, *et al*. cIAP2 promotes gallbladder cancer invasion and lymphangiogenesis by activating the NF-κB pathway. Cancer Sci 2017;108(6):1144–1156. doi:10.1111/cas.13236, PMID:28295868.

[19] Cai MY, Tong ZT, Zheng F, Liao YJ, Wang Y, Rao HL, *et al*. EZH2 protein: a promising immunomarker for the detection of hepatocellular carcinomas in liver needle biopsies. Gut 2011;60(7):967–976. doi:10.1136/gut.2010.231993, PMID:21330577.

[20] Liao Y, Wang C, Yang Z, Liu W, Yuan Y, Li K, *et al*. Dysregulated Sp1/miR-130b-3p/HOXA5 axis contributes to tumor angiogenesis and progression of hepatocellular carcinoma. Theranostics 2020;10(12):5209–5224. doi:10.7150/thno.43640, PMID:32373208.

[21] Wang C, Liao Y, He W, Zhang H, Zuo D, Liu W, *et al*. Elafin promotes tumour metastasis and attenuates the anti-metastatic effects of erlotinib via binding to EGFR in hepatocellular carcinoma. J Exp Clin Cancer Res 2021;40(1):113. doi:10.1186/s13046-021-01904-y, PMID:33771199.

[22] Chandrashekar DS, Bashel B, Balasubramanya SAH, Creighton CJ, Ponce-Rodriguez I, Chakravarthi BVSK, *et al*. UALCAN: A Portal for Facilitating Tumor Subgroup Gene Expression and Survival Analyses. Neoplasia 2017;19(8):649–658. doi:10.1016/j.neo.2017.05.002, PMID:28732212.

[23] Petit V, Thiery JP. Focal adhesions: structure and dynamics. Biol Cell 2000;92(7):477–494. doi:10.1016/s0248-4900(00)01101-1, PMID:11229600.

[24] Jiang XJ, Chen ZW, Zhao JF, Liao CX, Cai QH, Lin J. cIAP2 via NF-κB signalling affects cell proliferation and invasion in hepatocellular carcinoma. Life Sci 2021;266:118867. doi:10.1016/j.lfs.2020.118867, PMID:33310033.

[25] Fu PY, Hu B, Ma XL, Yang ZF, Yu MC, Sun HX, *et al*. New insight into BIRC3: A novel prognostic indicator and a potential therapeutic target for liver cancer. J Cell Biochem 2019;120(4):6035–6045. doi:10.1002/jcb.27890, PMID:30368883.

[26] Rada M, Nallanthighal S, Cha J, Ryan K, Sage J, Eldred C, *et al*. Inhibitor of apoptosis proteins (IAPs) mediate collagen type XI alpha 1-driven cisplatin resistance in ovarian cancer. Oncogene 2018;37(35):4809–4820. doi:10.1038/s41388-018-0297-x, PMID:29769618.

[27] Li L, Wang W, Li X, Gao T. Association of ECRG4 with PLK1, CDK4, PLOD1 and PLOD2 in esophageal squamous cell carcinoma. Am J Transl Res 2017;9(8):3741–3748. PMID:28861165.

[28] Provenzano PP, Eliceiri KW, Campbell JM, Inman DR, White JG, Keely PJ. Collagen reorganization at the tumor-stromal interface facilitates local invasion. BMC Med 2006;4(1):38. doi:10.1186/1741-7015-4-38, PMID:17190588.

[29] Levental KR, Yu H, Kass L, Lakins JN, Egeblad M, Erler JT, *et al*. Matrix crosslinking forces tumor progression by enhancing integrin signaling. Cell 2009;139(5):891–906. doi:10.1016/j.cell.2009.10.027, PMID:19931152.

[30] Zhu J, Xiong G, Fu H, Evers BM, Zhou BP, Xu R. Chaperone Hsp47 Drives Malignant Growth and Invasion by Modulating an ECM Gene Network. Cancer Res 2015;75(8):1580–1591. doi:10.1158/0008-5472.Can-14-1027, PMID:25744716.

[31] Wang D, Berglund A, Kenchappa RS, Forsyth PA, Mulé JJ, Etame AB. BIRC3 is a novel driver of therapeutic resistance in Glioblastoma. Sci Rep 2016;6:21710. doi:10.1038/srep21710, PMID:26888114.

[32] Avnet S, Chano T, Massa A, Bonuccelli G, Lemma S, Falzetti L, *et al*. Acid microenvironment promotes cell survival of human bone sarcoma through the activation of cIAP proteins and NF-κB pathway. Am J Cancer Res 2019;9(6):1127–1144. PMID:31285947.

[33] Gjaltema RAF, de Rond S, Rots MG, Bank RA. Procollagen Lysyl Hydroxylase 2 Expression Is Regulated by an Alternative Downstream Transforming Growth Factor β-1 Activation Mechanism. J Biol Chem 2015;290(47):28465–28476. doi:10.1074/jbc.M114.634311, PMID:26432637.

[34] Ikushima H, Negishi H, Taniguchi T. The IRF family transcription factors at the interface of innate and adaptive immune responses. Cold Spring Harb Symp Quant Biol 2013;78:105–116. doi:10.1101/sqb.2013.78.020321, PMID:24092468.